



## Significant advantages of the strontium oxide in glasses and glass ionomer cements (GICs)

Mohamed El Baiomy<sup>1\*</sup>, Gomaa El Damrawi<sup>1</sup>, and Rawya Mohammed Ramadan<sup>2</sup>.

<sup>1</sup> Faculty of Science, Physics Department, Mansoura University, 35516 Mansoura, Egypt

<sup>2</sup> Microwave Physics and Dielectrics Department, Physics Research Division, National Research Centre, 12622, Dokki, Cairo, Egypt

Corresponding author: [mohamedalicbc@gmail.com](mailto:mohamedalicbc@gmail.com)

Received: 21/ 5 /2021  
Accepted: 22/6/2021

**Abstract:** Oxide glasses and glass ionomer cements (GICs) in the  $x\text{SrO}-(45-x)\text{SiO}_2-24.5\text{CaO}-24.5\text{Na}_2\text{O}-6\text{P}_2\text{O}_5$ , (0 x 15 mol %) have been prepared and studied by several spectroscopic techniques. The structure of all obtained compositions was confirmed to be amorphous in nature. The bulk of the non-crystallized glasses were treated thermally at a specific temperature to activate the nucleation processes, which is suitable for the material to be used as scaffolds and implants. The GICs are prepared from two parts: powder and liquid. Strontium-silicate glass is present in the powder and the liquid is an aqueous poly (acrylic) acid solution. The state of GIC was checked up by both FTIR and NMR spectroscopy. The cement of strontium and calcium carboxyl groups are confirmed to be formed. NMR spectra suggest that the glass containing a significant amount of non-bridging oxygens NBOs can dissolve quickly in specific solutions and vice versa. GIC of chemical shift in the region of shielded silicate units (contains three bridging bonds) are confirmed to be formed. The shielded silicate units in the well-formed GIC prevent the material from corrosion and dissolutions in water. Consequently, the as-obtained GIC is recommended to be applied as restorative and or implants and scaffolds

**keywords:** amorphous, glass ionomer, Implants, dental glasses

### 1.Introduction

Some implanted materials are considered "bioactive" if they can form a tight and chemically stable bond with living bone. This property is present in some glass compositions. Glasses in the system  $\text{Na}_2\text{O}-\text{CaO}-\text{SiO}_2-\text{P}_2\text{O}_5$  reported by Hench et al [1] are the first material that posses some types of bonds which are compatible with bone without any fibrous tissue [2]. Recently, there are some types of oxide glasses and glass ceramics that can elicit an appropriate biological response and result in the formation of a bond with living tissues [3, 4].

New modified dental materials are derived from bioactive glass-ceramics, which have different structures and properties than standard glasses. For instance, glass ionomer cements (GICs) are utilized in restorative dentistry as

restorative materials. Because of their direct adhesion to tooth tissue, low setting shrinkage, and a coefficient of thermal expansion close to that of a tooth, glass ionomer cement (GICs) were first widely used in dentistry [5, 6]. GICs are made up of two parts: powder and liquid. Strontium (Sr) or calcium alumina-silicate ( $\text{CaO}-\text{SiO}_2-\text{Al}_2\text{O}_3$ ) glass is present in the powder. The liquid is the aqueous poly (acrylic) acid solution [7, 8].

GIC is currently used in dental implants as a scaffold, bone graft, and coating material. Some bioactive glasses can form HAP in a matter of hours and simply bind to tissues [9,10]. The majority of previous studies are based on  $\text{SiO}_2$  containing glasses as stronger glass formers [5,11, 12]. The importance of silicate glasses in stimulating gene activation and promoting

bone regeneration has been demonstrated [9]. Nucleating agents (NAs) such as  $\text{TiO}_2$ ,  $\text{Cr}_2\text{O}_3$ ,  $\text{V}_2\text{O}_5$ , and  $\text{SrO}$  can be used in the production of bioglass or glass-ceramics to induce bulk crystallization of the apatite phases [13,14]. The majority of these materials are based on amorphous silicate with a silicon dioxide 45S5® composition developed by Hench et al. [11].

Silicate glasses containing  $\text{SrO}$  substituting both  $\text{CaO}$  and  $\text{NaO}$  were prepared and characterized for their bioactivity or bone-bonding ability. Due to similar ionic size and polarity, ( $\text{Sr}^{2+}$ ) is accepted to function similarly to ( $\text{Ca}^{2+}$ ), and its role in bone metabolism has been extensively documented [15,16]. Since strontium is the most similar element to calcium, and glasses containing it were already being used in dental composite resin restoratives [17,18].  $\text{Sr}$  is beneficial biologically, specifically for healthy bone growth [19,20]. Strontium  $\text{Sr}$  has become a major global issue due to its influence on bone cells [21].  $\text{Sr}$  is an alkaline earth metal that, like  $\text{Ca}$ , helps to form bones.  $\text{Sr}$  can be found in the liver, muscles, and bodily fluids, but it is most abundant in bone [22,23]. Because there have been few studies on  $\text{SrO}$  containing GIC, this study aims to shed more light on the structural roles of  $\text{SrO}$  in glass, glass ceramics, and GIC.

## 2. Experimental details

### 2.1. Sample preparation

Glass samples were prepared from chemically pure Strontium Oxide ( $\text{SrO}$ , 99.9% Aldrich) which was used directly.  $\text{Na}_2\text{O}$  was introduced as sodium carbonate ( $\text{Na}_2\text{CO}_3$  (99%), purity), and  $\text{SiO}_2$  (99.8%), purity),  $\text{P}_2\text{O}_5$  as di-hydrogen orthophosphate ( $\text{NH}_4\text{H}_2\text{PO}_4$  (98%), purity), and  $\text{CaO}$  as calcium carbonate ( $\text{CaCO}_3$  (99%), purity). Glasses were prepared and obtained according to the molar composition  $x\text{SrO} - (45-x) \text{SiO}_2 - 24.5 \text{CaO} - 24.5 \text{Na}_2\text{O} - 6 \text{P}_2\text{O}_5$ , (0 x 15 mol %). (where  $x$  ranges from 0 to 40 mol %). The batches were precisely weighed before being melted in silica crucibles in an electric furnace at  $1150^\circ\text{C}$  for 45 minutes, and the melts were shocked several times to achieve homogeneity.

At room temperature, GICs were made by hand mixing the experimental glass powder and the acid solution on a poly (methyl methacrylate) (PMMA) mixing plate with a polyethylene (PE) spatula (SciLabware Ltd, Staffordshire). The size of glass particles has a significant impact on their performance when mixed with polymer liquid (polyacrylic acid). GICs are frequently delivered as a powder containing their own liquid. The powder is made of modified strontium silicate glass, and the liquid is an aqueous solution of a polyalkenes acid, such as polyacrylic acid; however, in later formulations, the acid may be added to the powder in the form of a dried polymer.

### 2.2. Experimental Techniques

For X-ray diffraction measurements, a Shimadzu X-ray diffractometer is used (the apparatus type Dx-30, Metallurgy institute, El Tebbin, Cairo, Egypt). The maximum peak and intensity values are used to determine the material type, which is compared to patterns in the international powder diffraction file (PDF) database of the joint committee for powder diffraction standards (JCPDS).

**Table 1.** Compositions (mol%) of the prepared samples of the formula  $x\text{SrO} - (45-x) \text{SiO}_2 - 24.5\text{CaO} - 24.5\text{Na}_2\text{O} - 6\text{P}_2\text{O}_5$ .

Sample	SiO2	CaO	Na2O	P2O5	SrO
Sr0	45	24.5	24.5	6	0
Sr3	42	24.5	24.5	6	3
Sr5	40	24.5	24.5	6	5
Sr10	35	24.5	24.5	6	10
Sr15	30	24.5	24.5	6	15

Using a Mattson 5000 FTIR spectrometer, the spectra are measured in the  $400 - 4000 \text{ cm}^{-1}$  range with a spectral resolution of 2 cm. The resulting spectrum was normalized to that of a blank KBr pellet and corrected for background and dark currents using a two-point baseline. The normalization is necessary to eliminate the concentration effect of the powder sample in the KBr disc.

The JEOL GSX-500 high-resolution solid-state MAS NMR spectrometer with a magnetic field of 11.74 T was used to analyze finely powdered samples of various compositions (Mansoura University, Mansoura, Egypt). At a frequency of 99.3 MHz, the spectra of silicon nuclei were observed. Using a

zirconia sample holder, a spinning rate of 7 kHz was applied. A 2.62-second electric pulse with a 30 second recycle delay is used. To obtain high-resolution NMR spectra, several scans (10,000 - 12,000) were performed.

### 3. Results and Discussion

Figure 1 depicts the XRD pattern of two selected samples of different glass compositions. In the measured spectra, no crystallization peaks can be found. As a result of the measured XRD spectra, a completely amorphous structure was assumed. The amorphous bio-silicate glasses have the advantage of being highly desirable as a scaffold material. This is due to the ability of amorphous glasses to produce different bioactive pour layers. On the other hand, the crystallization process reduces glass's bioactivity [27]. This is due to the fact that a crystalline structure is responsible for a closed glass network with limited pores, which causes a glass to be solid, less soluble, and less reactive. As a result, crystalline glass was not further characterized or used to fabricate scaffolds. However, it is preferred in both orthodontic and orthopedic applications. To use modified silicate glasses as a scaffold, the crystallization limit should be reduced, and the capacity of nucleating bio-nuclei should be extremely high. To achieve a balance between the two extremes, the material is thermally treated to enhance the nucleating process, which increases material dissolution while keeping the network amorphous. These processes are regarded as the primary feature that serves the material as a scaffold. The greater the nucleating network, the more pores in the structure that are suitable for scaffold state. According to their DSC curves [24], the materials were thermally treated at a temperature just below the T<sub>g</sub> region (T<sub>g</sub> around 530°C) to enhance the nucleation process of the well-formed biomolecules.

FTIR was used to structurally characterize bioactive glasses and scaffolds in order to determine their chemical composition and to confirm the presence of non-bridging active P-O and Si-O groups, which influence glass bioactivity. The data from the FTIR absorbance spectroscopy of the glass molecules revealed

main peaks centered at approximately 500, 575, 780, 920, and 1040 cm<sup>-1</sup> (figure 2 ). The presence of an a-Si-O bond with mixed one and two non-bridging oxygen per SiO<sub>4</sub> tetrahedron was suggested by the peak in the 850–1000 cm<sup>-1</sup> range [25,26]. This suggests that the glass containing a significant amount of NBOs can dissolve quickly in specific solutions. Previous research has suggested that the peak at 500–600 cm<sup>-1</sup> in high phosphate-containing glasses corresponds to the P-O bending mode as well as a Si-O-Si bending vibration in this region [27, 28]. The peak at 750 cm<sup>-1</sup> is caused by 4 NBO in both silicate and phosphate networks [29,30]. The Si-O stretching vibration of three BO in SiO<sub>4</sub> tetrahedral units is responsible for the absorption beak around 1150 cm<sup>-1</sup> [29,31]. Table 2 summarizes the assignments for each of the FTIR bands.

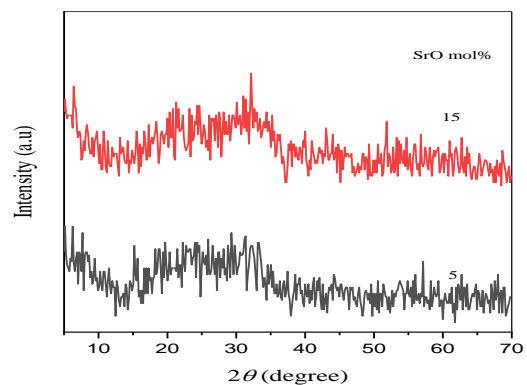


**Figure 1.** XRD patterns of two compositions (5 and 15 mol% SrO) treated thermally just below T<sub>g</sub> (500 °C, 2 hours) to enhance the nucleation process of the well-formed biomolecules.

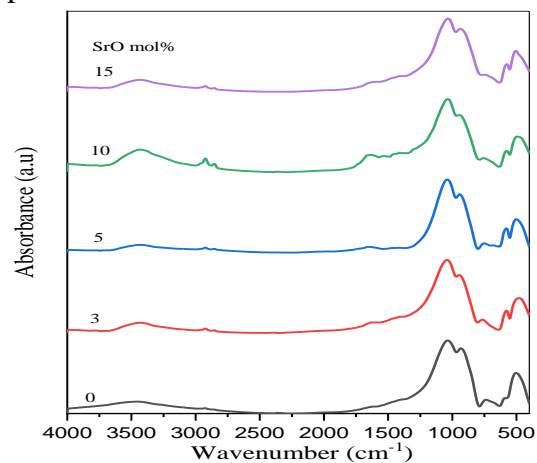


**Figure 2.** FTIR spectra for as prepared glasses containing 0, 5, 10, and 15 mol% SrO.

The deconvolution of FTIR spectra for two glass samples was shown in Fig. 3 (a, b), and

the de-convolution parameters for all studied samples were calculated.

**Table. 2** Assignments for different FTIR absorption bands of the studied glass.

	Reference
500–600 $\text{cm}^{-1}$ corresponds to the P–O bending mode as well as a Si–O–Si bending vibration in this region	[27,28]
850–1000 $\text{cm}^{-1}$ suggested the presence of a Si–O bond with mixed one and two non-bridging oxygen per $\text{SiO}_4$ tetrahedron	[25,26]
The peak around 750 $\text{cm}^{-1}$ is due to 4 NBO both in silicate and phosphate networks.	[29,30]
The absorption beak around 1150 $\text{cm}^{-1}$ is assigned to the S-O stretching vibration of three BO in $\text{SiO}_4$ tetrahedral units.	[29,31]

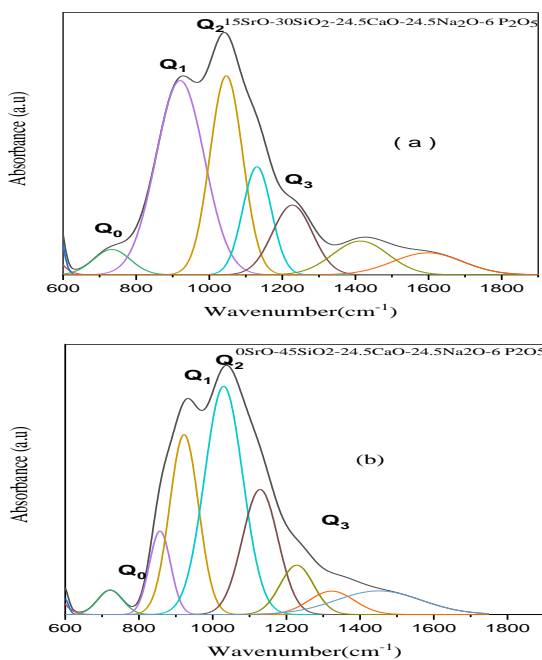


**Figure 3.** (a, b) The deconvolution of the experimental spectra for sample containing (Sr0 & Sr15)

Figure 4 depicts the FTIR spectra of both glasses following and prior to the reaction with organic polymeric acid. The cement phase appears in the glass only after the reaction process has been completed. The presence of new splitting absorbance peaks around 1500  $\text{cm}^{-1}$  identifies cement species. Because of the acid-base reaction, the cement phase is only present in the glass after the acid-base reaction.

The surface of the glass changes into a silica hydrogel (Si-OH). The unreacted cores of the glass particles serve as a filler. The self-cure polymerization reaction is then initiated by combining GIC powder and liquids

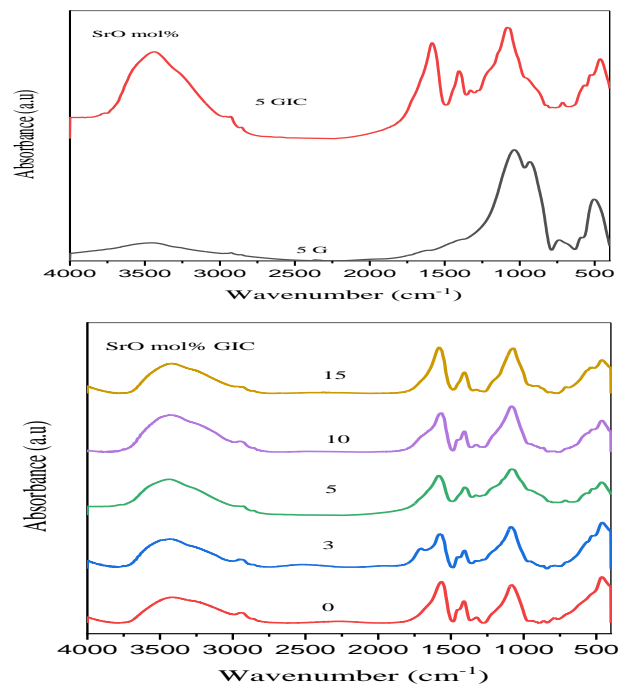


**Figure 4.** FTIR spectra of both glass and GICs concentration mol% SrO.

NMR results from the same glasses provide additional evidence for acid-base reaction. Figures 5. The analysis of the spectra of (figure 5) is represented by Figure 6 which shows that the acid-base reaction has a significant impact on the NMR resonance peaks. The degradation processes cause an increase in the resonance NMR peaks. These changes are regarded as strong evidence for degradation processes that are simply the result of the reaction between the glass and the acid [20].

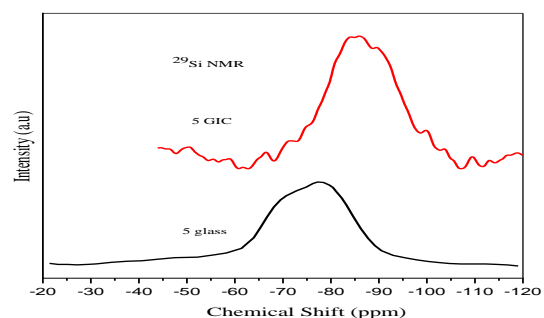


**Figure 5.**  $^{29}\text{Si}$  NMR of 5SrO-40SiO<sub>2</sub> glass and GIC.

Figure 6(a, b) is the deconvoluted NMR spectra of the analyzed compositions. There are different values of the chemical shift of silicate nuclei which are observed in spectra of the investigated glasses. The isotropic chemical shift of glass containing SrO is listed at about -64, -72.15, and -83.5 ppm. These values are assigned to a mixture of Q<sub>1</sub>, Q<sub>2</sub>, and Q<sub>3</sub> groups [28-31]. Where Q<sub>1</sub> is referred to as silicate tetrahedral units containing only one bridging oxygen atom (BO), Q<sub>2</sub> means two NBO atoms are formed per SiO<sub>4</sub> tetrahedral units and Q<sub>3</sub> means three NBO atoms are formed per SiO<sub>4</sub> tetrahedral units. On the other hand, the values of the chemical shift were decreased upon acid-base reaction. It can be shown from figure 2(b) that the corresponding values of the chemical shift appear at -68.4, which confirms that Q<sub>4</sub> configurations are formed via the presence of an acid-base reaction. The formation of more shielded silicate units as a direct result of the acid-base reaction is responsible for this shift.

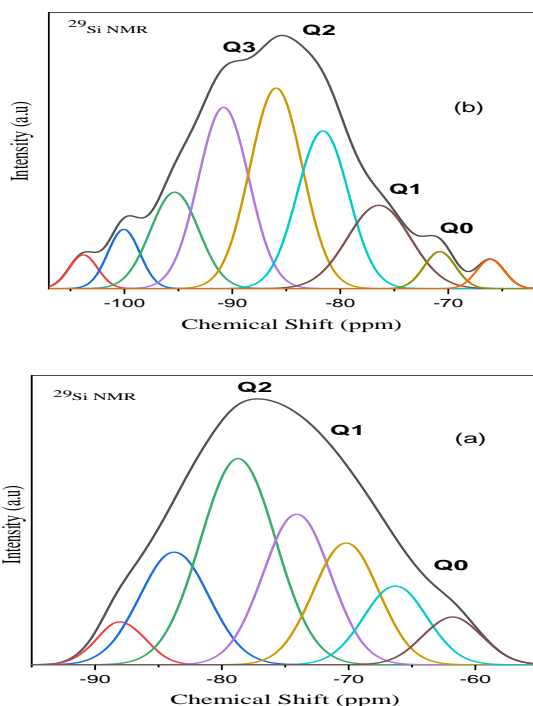


**Figure.6** Deconvoluted spectra of glass(a)&GIC (b) containing 5 mol% SrO.

#### 4. Conclusion

GICs in the xSrO - (45-x)SiO<sub>2</sub> - 24.5CaO - 24.5Na<sub>2</sub>O - 6 P<sub>2</sub>O<sub>5</sub>, (x= 0 to 15 mol %) were prepared and studied. The structure of all

obtained compositions was confirmed to be amorphous in nature. The as-obtained glasses were treated thermally at a specific temperature to activate the nucleation processes. The GICs are prepared from the inorganic powder and the organic liquid. The state of GIC was checked up by both FTIR and NMR spectroscopy. The cement of Sr and Ca carboxyl groups are confirmed to be formed. NMR spectra suggest that the glass containing a significant amount of NBOs can dissolve quickly in specific solutions and vice versa.

#### 4. References

1. Bajda, S., et al., (2021), Laser cladding of bioactive glass coating on pure titanium substrate with highly refined grain structure. *Journal of the Mechanical Behavior of Biomedical Materials*,: **119**, p. 104519.
2. Bairo, F. and E. Fiume, (2020)3D printing of hierarchical scaffolds based on mesoporous bioactive glasses (MBGs)—Fundamentals and applications. *Materials*, **13**(7): p. 1688.
3. Preethi, M.,( 2020), Comparison of Physical Characteristics of Moldable Calcium Phosphate Bone Grafts with Commercially Available Moldable Bone Grafts used in Surgical Periodontal Therapy: An In Vitro Study. Vivekanandha Dental College for Women, Tiruchengode, *MASTER OF DENTAL SURGERY, Department of Periodontics, Vivekanandha Dental College for Women, Tiruchengode*.
4. Uskoković, V., et al., (2021)Synthesis and characterization of nanoparticulate niobium-and zinc-doped bioglass-ceramic/chitosan hybrids for dental applications. *Journal of Sol-Gel Science and Technology*,. **97**(2): p. 245-258.
5. Tiskaya, M., et al., (2021). The use of bioactive glass (BAG) in dental composites: A critical review. *Dental Materials*,. **37**(2): 296-310.
6. Khiri, M.Z.A., et al., (2020)Soda lime silicate glass and clam Shell act as precursor in synthesize calcium fluoroaluminosilicate glass to fabricate glass ionomer cement with different ageing time. *Journal of Materials Research and Technology*,. **9**(3): p. 6125-6134.

7. Alamri, A., et al., (2020). The Effect of Bioactive Glass-Enhanced Orthodontic Bonding Resins on Prevention of Demineralization: A Systematic Review. *Molecules*, **25**(11): p. 2495.
8. Fada, R., et al., (2021) Mechanical properties improvement and bone regeneration of calcium phosphate bone cement, Polymethyl methacrylate and glass ionomer. *Journal of Nanoanalysis*, **8**(1): p. 60-79.
9. Yang, Z., et al., (2020). Nanotechnology in Dental Therapy and Oral Tissue Regeneration, in Nanotechnology in Regenerative Medicine and Drug Delivery Therapy. *Springer*. p. 91-189.
10. Rezaie, H.R., et al., (2020) Dental Restorative Materials, in A Review on Dental Materials., *Springer*. p. 47-171.
11. Pedone, A., V. Cannillo, and M.C. Menziani, (2021). Toward the Understanding of Crystallization, Mechanical Properties and Reactivity of Multicomponent Bioactive Glasses. *Acta Materialia*, **213**, 116977.
12. Davaie, S., T. Hooshmand, and S. Ansarifard, (2021). Different types of bioceramics as dental pulp capping materials: A systematic review. *Ceramics International*, **15**, p. 20781-20792
13. Karan, R., et al., (2021) Structure, properties and in-vitro response of SiO<sub>2</sub>-Na<sub>2</sub>O-CaO-P<sub>2</sub>O<sub>5</sub> system based glass-ceramics after partial replacement of Na<sub>2</sub>O by Li<sub>2</sub>O. *Journal of Non-Crystalline Solids*, **556**: p. 120554.
14. Mahato, A., et al., (2021) Role of calcium phosphate and bioactive glass coating on in vivo bone healing of new Mg-Zn-Ca implant. *Journal of Materials Science: Materials in Medicine*, **32**(5): p. 1-20.
15. Spicer, C.D., (2020) Hydrogel scaffolds for tissue engineering: the importance of polymer choice. *Polymer Chemistry*, **11**(2): p. 184-219.
16. Aksoy, U.B., (2020). Archaeometric studies on selected samples of human bones excavated from the ruins of the roman amphitheatre in İznik. A THESIS SUBMITTED TO THE GRADUATE SCHOOL OF NATURAL AND APPLIED SCIENCES OF MIDDLE EAST TECHNICAL UNIVERSITY.
17. Huang, Y., et al., (2021). Dental Restorative Materials for Elderly Populations. *Polymers*, **13**(5): p. 828.
18. Mokhtari, S., (2020), Development of Novel Copper Glass Containing Bone Adhesives for Orthopaedic Applications: Structural, Mechanical, and Biological Evaluation. *New York State College of Ceramics at Alfred University. Inamori School*.
19. Demirel, M. and A.I. Kaya, (2020) Effect of strontium-containing compounds on bone grafts. *Journal of Materials Science*, **55**(15): p. 6305-6329.
20. Cirillo, M., et al., (2021) Strontium substituted hydroxyapatite with  $\beta$ -lactam integrin agonists to enhance mesenchymal cells adhesion and to promote bone regeneration. *Colloids and Surfaces B: Biointerfaces*, **200**: p. 111580.
21. Zhang, S., et al., (2020) Recent developments in strontium-based biocomposites for bone regeneration. *Journal of Artificial Organs*, p. 1-12.
22. Ciosek, Z., et al., (2021) The Effects of Calcium, Magnesium, Phosphorus, Fluoride, and Lead on Bone Tissue. *Biomolecules*, **11**(4): p. 506.
23. Elumalai, A., (2020). Using Strontium Coated Clay Nanoparticles For Bone Regeneration And Other Biomedical Applications. *Doctoral Dissertations, 847, Louisiana University*.
24. El-Damrawi, G. and R. Ramadan, (2021) Structural Role of Strontium Oxide in Modified Silicate Glasses. *Spernger Link*, **14**, p 4879-4885.
25. Patel, K.B., et al., (2021). Characterization of immiscibility in calcium borosilicates used for the immobilization of Mo<sup>6+</sup> under Au-irradiation. *Journal of the American Ceramic Society*, **104**(7): p. 3632-3651.
26. Kob, W. and S. Ispas, (2021). First-principles Simulations of Glass-formers. *Encyclopedia of Glass Science, Technology, History, and Culture*, p. 233-243.
27. Zhou, H., et al., (2021). An important Calcium Phosphate Compound-Its

- Synthesis, Properties and Applications in Orthopedics. *Acta Biomaterialia*,. **127**:41-55. doi: 10.1016/j.actbio.2021.03.050.
28. Yan, Y., et al., (2021) *Atomic layer deposition SiO<sub>2</sub> films over dental ZrO<sub>2</sub> towards strong adhesive to resin. Journal of the Mechanical Behavior of Biomedical Materials*,. **114**: p. 104197.
  29. Liu, C., et al., (2021) Quantification of phosphorus structures in CaO–SiO<sub>2</sub>–P<sub>2</sub>O<sub>5</sub> glasses via Raman spectroscopy. *Journal of Non-Crystalline Solids*,. **560**: p. 120579.
  30. Tainio, J., et al., (2020). Structure and in vitro dissolution of Mg and Sr containing borosilicate bioactive glasses for bone tissue engineering. *Journal of Non-Crystalline Solids*, **533**: p. 119893.
  31. Oueslati-Omrani, R. and A.H. Hamzaoui, (2020). Effect of ZnO incorporation on the structural, thermal and optical properties of phosphate based silicate glasses. *Materials Chemistry and Physics*, **242**: p. 122461.